Origin of electron spin-orbit anisotropy in pyramidal InAs quantum dots

C. Segarra, J. Planelles,* and J. I. Climente
Departament de Química Física i Analítica, Universitat Jaume I, Castelló de la Plana, Spain
(Dated: March 17, 2014)

We investigate the influence of quantum dot shape, composition and height on the spin-orbit interaction anisotropy of pyramidal InAs quantum dots using a fully three-dimensional Hamiltonian. The dependence of the spin-orbit interaction strength on the orientation of in-plane magnetic fields is consistent with the experiments reported by Takahashi *et al.* [Phys. Rev. Lett. **104**, 246801 (2010)], and it can be explained from the interplay between Rashba and Dresselhaus spin-orbit terms in dots with shape anisotropy. Our calculations reveal that the composition and the height of the dot have a major influence in determining the magnitude of the spin-orbit anisotropy.

PACS numbers:
Keywords: Spin-orbit interaction, Quantum dot, Magnetic field

I. INTRODUCTION

In recent years, spin physics has become one of the most active branches in condensed matter physics due to its promising applications.[1] In particular, spin-orbit interaction (SOI) has been intensively investigated in semiconductor quantum dots (QDs)[2], in which confinement hinders many decoherence mechanisms and leads to long-lived spin states[3, 4]. This makes these systems good candidates for spin-based technological applications in spintronics[5] and quantum information.[6]

For electrons in zinc-blende semiconductor QDs, the most important mechanisms of SOI are known to be Rashba SOI[7], resulting from the structure inversion asymmetry, and Dresselhaus SOI[8], resulting from the bulk inversion asymmetry of the material itself. The Hamiltonians that describe both Rashba and Dresselhaus SOI present intrinsic anisotropy. A good understanding of such anisotropy is crucial to control and manipulate single electron spins via external electric or magnetic fields. One way to probe it is through examination of the spin anticrossings in the energy level spectrum, whose magnitude is proportional to the SOI intensity.[9–11] Taking profit of this, Takahashi and co-workers recently investigated SOI in self-assembled InAs QDs.[12] The choice of InAs is particularly interesting because of the strong SOI of this material, which makes it convenient for spin manipulation via external fields. Indeed, the possibility of controlling single spin-states in these systems has been demonstrated both electrically[13] and magnetically.[12]

The experiment of Takahashi et al. showed that electrons in InAs QDs present pronounced in-plane SOI anisotropy. To this end, they used an in-plane magnetic field, whose direction was rotated over all possible azimuthal angles, ϕ. It was found that the angular dependence of the SOI strength fits the form of an absolute cosine function with an offset ϕ_0, $|\cos(\phi - \phi_0)|$. The origin of this dependence was tentatively ascribed to the QD elongated geometry along with the contribution of Rashba SOI.[12] Soon after, a theoretical work by Nowak et al. proposed an alternative explanation. They ascribed the origin of the offset to the combined action of Rashba and Dresselhaus SOI in elongated QDs.[14] This conclusion was based on a single-electron effective mass model where QDs are represented as simple cuboids and that the confinement potential is separable, namely, $V(r) = V_x(x) + V_y(y) + V_z(z)$. Because recent evidences have demonstrated that a realistic three-dimensional confinement is required for quantitative understanding of the SOI properties,[15, 16] one wonders to which extent this finding holds in the actual pyramidal-shaped QDs of the experiment.

In this work, we provide new insight on the origin of the SOI anisotropy in self-assembled InAs QDs. This is done by using fully three dimensional effective mass Hamiltonians, with inclusion of both Rashba and Dresselhaus SOI, electric and magnetic fields, and accurate modeling of the pyramidal QD structure. We find that Rashba or Dresselhaus interaction alone do not explain the presence of the offset ϕ_0 in the angular magnetic field dependence even if the QD is anisotropic. Rather, it arises from the simultaneous presence of the two SOI terms, which supports the interpretation Nowak and co-workers obtained with cuboidal QDs.[14] With this result in mind, we next explore the effect of the QD height and composition. Because the height and the (In,Ga) composition have a strong influence on the magnitude of Dresselhaus and Rashba SOI, respectively, changing these structural parameters severely affects the balance between the two SOI terms. As a result, the magnitude of the angular offset rapidly decreases with increasing QD height and Ga composition.

II. THEORY

We study the conduction band electronic structure of semiconductor QDs within the effective mass and envelope function approximations. The three-dimensional

*Electronic address: josep.planelles@uji.es

single-electron Hamiltonian reads

$$H = \frac{\mathbf{p}^2}{2m^*} + V(\mathbf{r}) - \mathbf{E}\,\mathbf{r} + H_Z + H_R + H_D \qquad (1)$$

where m^* stands for the electron effective mass, $\mathbf{p} = -i\hbar\boldsymbol{\nabla} + \mathbf{A}$ is the canonical momentum operator and $V(\mathbf{r})$ is the confining potential. Following the setup of Ref. 12, a magnetic field oriented in the xy plane and rotated an angle ϕ with respect to the x axis is also included. Such a magnetic field has the form $\mathbf{B} = B\,(\cos\phi, \sin\phi, 0)$ and is described by the vector potential $\mathbf{A} = (zB\sin\phi, -zB\cos\phi, 0)$. The third term accounts for an externally applied electric field, which is directed along z in the experiments. Thus, $\mathbf{E} = (0, 0, E_z)$.

We also introduce the Zeeman term

$$H_Z = \frac{1}{2} g \mu_B \mathbf{B}\,\boldsymbol{\sigma} \qquad (2)$$

where $\boldsymbol{\sigma}$ are the Pauli spin matrices, μ_B is the Bohr magneton and g is the electron g-factor.

The last two terms in Eq. (1) are additional terms resulting from the SOI.[17] The Rashba SOI is described by the Hamiltonian

$$H_R = r\,E_z\,(\sigma_x\,p_y - \sigma_y\,p_x). \qquad (3)$$

and the Dresselhaus SOI by the Hamiltonian

$$H_D = d\left[\sigma_x p_x\left(p_y^2 - p_z^2\right) + \sigma_y p_y\left(p_z^2 - p_x^2\right) + \sigma_z p_z\left(p_x^2 - p_y^2\right)\right] \qquad (4)$$

Here, r and d are material-dependent coefficients determining the strength of the SOI.

The eigenvalue equation of Hamiltonian (1) is solved numerically using a finite-difference method on a three-dimensional grid.

III. RESULTS AND DISCUSSION

The system we consider is represented in Fig. 1. It consists of a pyramidal InAs QD similar to that used in Ref. 12. The QD is grown on top of a GaAs wetting layer and is uncapped. Because the surface of uncapped QDs is usually oxidized, the tip can be considered as insulating and the QD is better described as a truncated pyramid.[18] The base of the QD is rectangular due to the electrostatic confinement induced by the side gates. We assume the elongated direction (x axis) is along the [100] crystalographic axis.

Our first target is to understand the origin of the SOI angular dependence. Following Ref. 12 experiment, this is estimated from the magnitude of the spin anticrossing gap between the s-shell and p-shell for different orientations of the magnetic field. The confining potential is defined by the conduction band offset between InAs and GaAs, $V_{InAs/GaAs} = 0.69\,eV$[19], and the vacuum is treated by using a high potential barrier, $V_{vacuum} = 4\,eV$. A uniform composition of 66% In is assumed inside the QD, which takes into account the diffusion of Ga into the otherwise pure InAs material. Similar alloy compositions have been experimentally observed in other epitaxially grown InAs QDs.[20, 21] The electron effective mass and the SOI coefficients are calculated using linear interpolation from the pure InAs and GaAs parameters [17, 19]. The values used in the simulations are $m^* = 0.04\,m_0$ (m_0 is the free electron mass), $r = 79.0\,e\mathring{A}^2$ and $d = 27.32\,eV\mathring{A}^3$.

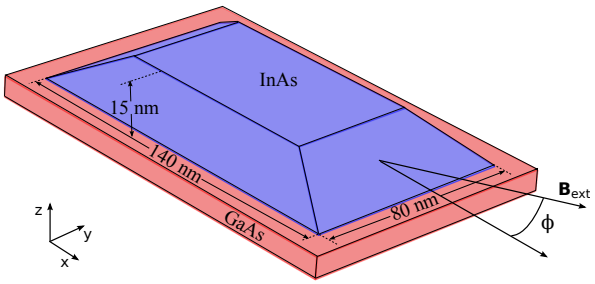

FIG. 1: Schematic representation of the uncapped InAs QD system. The dimensions of the QD considered in the simulations and the orientation of the magnetic field are also indicated. The upper base of the pyramid is 0.6 times the lower one.

The magnitude of the electric field in the QD is roughly estimated to be $E_z = -15KV/cm$,[22] and we use this value in all our calculations. For the g-factor, we take the experimental value, $g = -4.1$, much smaller than the bulk value used in Ref. 14. This shifts the spin anticrossing under study towards higher magnetic fields. Indeed, the dimensions and composition of the QD in Fig. 1 have been adjusted in order to match the magnetic field at which the anticrossing takes place in the experiment. Using the experimentally inferred g-factor is also consistent with recent work showing that the bulk g-factor is strongly reduced by quantum confinement.[23]

A. SOI angular dependence

Fig. 2 illustrates the electron energy levels under an in-plane magnetic field oriented along the x direction ($\phi = 0$). When the SOI is not included, the lowest spin-down state and the first excited spin-up state can cross (see dashed rectangle). As mentioned above, the dimensions and composition of our QD are fitted to reproduce the experimental field of the anticrossing, $B_{AC} \approx 11.5\,T$. On doing this, we also reproduce the experimental anticrossing field for B aligned along y ($\phi = 90$), which takes place at $B_{AC} \approx 10\,T$ due to the stronger confinement –not shown–.[22]

When SOI is included, the intersection of the states

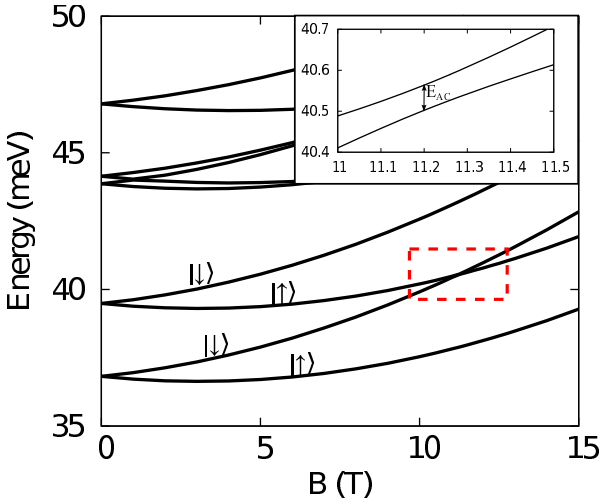

FIG. 2: Electron energy spectrum as a function of the magnetic field in absence of SOI. The magnetic field is oriented in the x direction, $\phi = 0$. The crossing of electron states we examine is pointed out by the dashed red box. Inset: avoided crossing when both Dresselhaus and Rashba SOI are present.

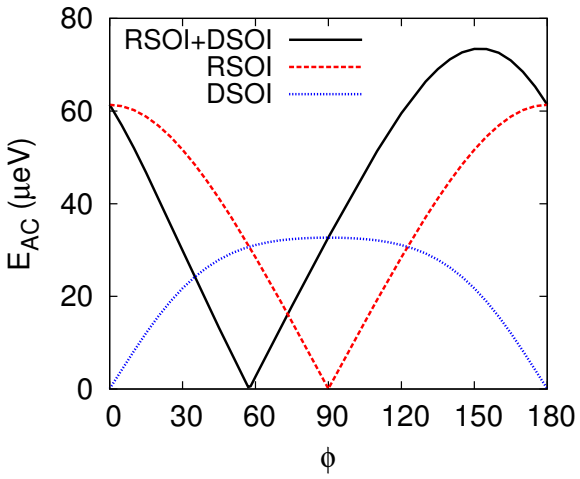

FIG. 3: Anticrossing energy E_{AC} as a function of the in-plane magnetic field orientation ϕ. Results including only Dresselhaus SOI (blue dotted line), only Rashba SOI (red dashed line) and both Dresselhaus and Rashba SOI (black solid line) are presented.

we consider turns into an anticrossing. The inset of Fig. 2 shows the anticrossing formed in the presence of SOI. We define the anticrossing energy E_{AC} as the minimal separation between the two states at the avoided crossing.

In Fig. 3, we show the magnitude of the anticrossing energy when the two SOI mechanisms are present individually and also simultaneously. In all three cases, there is a clear dependency between E_{AC} and the magnetic field orientation revealing the SOI anisotropy. When only Rashba SOI is present, the anticrossing is maximum for **B** is oriented parallel to the x axis ($\phi = 0$) and it decreases with the rotation of **B** until it cancels out at $\phi = 90$. For this orientation, the SOI quenches and the states cross. For Dresselhaus SOI the behavior is the opposite instead. E_{AC} is zero at $\phi = 0$ and it becomes maximum at $\phi = 90$. The results in Fig. 3 can be fitted well by the absolute value of a cosine (sine) function for the Rashba (Dresselhaus) SOI.

When both contributions are present at the same time, the anticrossing energy has a similar form compared with the single SOI cases, but the singular points are no longer found when **B** is aligned with the principal axes of the dot. In this case, the minimum appears at $\phi \approx 57$ and the maximum at $\phi \approx 147$. Note that the curve including both terms can be obtained qualitatively as the absolute value of the subtraction (addition) of the individual curves for $0 < \phi < 90$ ($90 < \phi < 180$). Then, the minimum takes place at $0 < \phi < 90$ when the two single SOI curves cross since the two terms cancel each other out. The results can be fitted by the absolute value of a cosine function with an offset ϕ_0, $E_{AC} \propto |cos(\phi - \phi_0)|$. The extent of ϕ_0 is determined by the relative strength of the Rashba and Dresselhaus SOI contributions. In the limit of Rashba SOI only, $\phi_0 = 0$, and in the limit of Dresselhaus SOI only, $\phi_0 = 90$.

Fig. 3 shows that the finite value of ϕ_0 observed in experiments[12] can only occur when both SOI terms are present simultaneously. This result confirms that the explanation given by Nowak et al.[14] for cuboidal QDs holds also in more realistic geometries.

Determining the precise value of ϕ_0 in a QD thus depends on the balance between Rashba and Dresselhaus SOI terms. Obviously, knowledge on the angle where the two SOI terms cancel out is of interest for spin control and enhanced spin lifetimes.[24] Therefore, detailed understanding on the structural parameters affecting its value is desirable. One can see from Hamiltonians (3) and (4) that rotating the anisotropic confinement potential of the QD with respect to the crystallographic axes leads to changes in the weight of the SOI terms. This was shown to be an important control parameter of the SOI anisotropy in Ref. 14. In what follows, we discuss two additional factors which are equally important, namely the diffusion of Ga into the InAs dot and the height of the dot.

B. Dependence on the QD composition

Self-assembled InAs/GaAs QDs experience substantial diffusion of Ga from the GaAs matrix into the InAs islands during the growth process, which leads to significant variations in the QD compostion.[20, 21, 25] In this section we investigate how this affects the SOI anisotropy. Four InGaAs alloys with a uniform concentration, ranging from 50% In to 100% In, are considered. The results including both Rashba and Dresselhaus SOI are summarized in Fig. 4. As can be seen, decreasing the In con-

centration not only visibly reduces the magnitude of the spin anticrossings gap E_{AC} but it also reduces the angle where the two SOI terms cancel out.

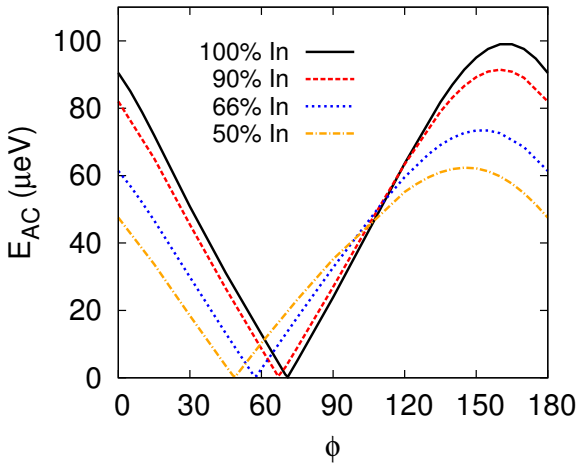

FIG. 4: Anticrossing energy vs. magnetic field orientation with both SOI contributions present. Results for different QD compositions are showed: 100% In (black solid line), 90% In (red dashed line, 66% In (blue dotted line) and 50% In (orange dash-dotted line).

This result can be understood considering the value of Rashba and Dresselhaus parameters of the pure materials. InAs and GaAs parameters for Dresselhaus SOI are similar ($d_{InAs} = 27.18\,eV\mathring{A}^3$ and $d_{GaAs} = 27.58\,eV\mathring{A}^3$).[17] Thus, the contribution of this term remains approximately the same for all InAs/GaAs alloys. By contrast, the parameters for Rashba SOI are very different ($d_{InAs} = 117.1\,e\mathring{A}^2$ and $d_{GaAs} = 5.026\,e\mathring{A}^2$)[17] so that the strength of the Rashba term decreases with decreasing In composition. As a consequence, Ga diffusion shifts the zero SOI angle towards the Dresselhaus limit, $\phi = 0$.

C. Effect of the QD height

We next explore the influence of the QD height on the anticrossing gap. The results, sumarized in Fig. 5, compare the SOI anisotropy of the QD studied so far (where the height is $L_z = 15\,nm$), with a shorter ($L_z = 10\,nm$) and a taller ($L_z = 20\,nm$) QD. We can see in this figure that while the global shape of the SOI dependence on the magnetic field does not change with the height, the anticrossing gap and the zero SOI angle do change. In particular, with increasing height the magnitude of E_{AC} decreases with L_z while the zero SOI angle increases.

This behavior can be qualitatively understood by considering the QD as a quasi-2D structure, where confinement along z is much stronger than that in the xy plane. One can then separate adiabatically the in-plane and vertical motions. By considering that only the lowest z state contributes to the low-energy spectrum, and integrating over this degree of freedom, the Dresselhaus Hamiltonian of Eq. (4) simplifies to:

$$H_D = d\,\langle p_z^2\rangle\,(\sigma_y p_y - \sigma_x p_x)\,. \tag{5}$$

where we have assumed $\langle p_z\rangle = 0$ and neglected terms which do not involve $\langle p_z^2\rangle$. Because $\langle p_z^2\rangle \propto 1/L_z^2$, Eq. (5) reveals that the Dresselhaus SOI term tends to decrease with QD height. By contrast, the height barely affects the Rashba SOI term, see Eq. (3). As a result, increasing L_z reduces the overall SOI strength and shifts the zero SOI angle towards the Rashba SOI limit, $\phi = 90$.

It is worth pointing out that the results of Fig. 5 are obtained with a fully 3D, cubic Dresselhaus Hamiltonian, without the approximations of Eq. (5). This is important for a quantitative analysis, as the strong magnetic fields where spin anticrossings take place ($B \approx 10\,T$) already imply comparable magnetic and spatial confinement in the growth direction. This has been found to affect the electron SOI anisotropy in related systems.[24]

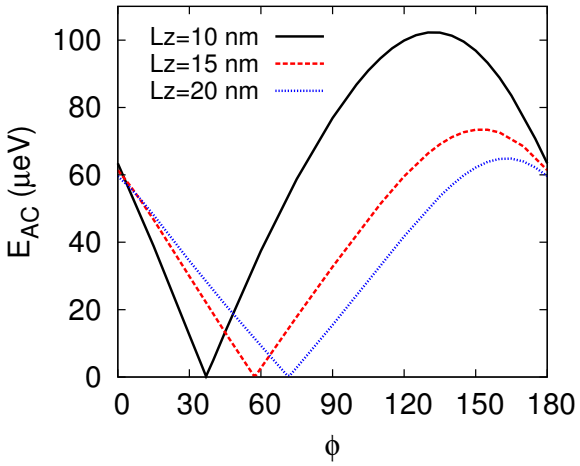

FIG. 5: Anticrossing energy as a function of the magnetic field orientation with both SOI. Results for a QD height of 20nm (blue dotted line), 15nm (red dashed line) and 10nm (black solid line) are presented.

IV. CONCLUSIONS

We have investigated the SOI anisotropy in single uncapped InAs QDs subject to in-plane magnetic fields. Using a three-dimensional model, we described the system with a realistic truncated pyramid geometry. It was found that the SOI strength oscillates with the magnetic field orientation, showing a complete suppression at a certain angle deviating from the main crystallographic axes, as noted in Ref. 12 experiment. This suppression can be explained from the compensation between Rasbha and Dresselhaus SOI terms.

We showed that the dot height and composition allow one to tune the Dresselhaus (Rashba) SOI strength over a wide range of values. This affects the Dresselhaus to Rashba SOI strenght ratio, yielding significant changes on the overall SOI intensity and the cancelation angles. Since the amount of Ga diffusion into the self-assembled QDs can be controlled through the growth temperature[25] and the QD height can be controlled using e.g. In flux techniques,[26] the two parameters offer an excellent control knob to tailor the SOI anistropy of self-assembled QDs.

Acknowledgments

This work was supported by UJI-Bancaixa Project No. P1-1B2011-01, MINECO Project No. CTQ2011-27324, and FPU Grant (C.S.).

[1] D. D. Awschalom, D. Loss and N. Samarth *Semiconductor Spintronics and Quantum Computing* (Springer, New York, 2002)
[2] R. Hanson, J. R. Petta, S. Tarucha and L. M. K. Vandersypen *Rev. Mod. Phys.* **79**, 1217 (2007)
[3] A. Khaetskii and Y. Nazarov, *Phys. Rev. B* (2000)
[4] M. W. Wu, J. H. Jiang, M. Q. Weng, *Phys. Rep.* **493**, 61 (2010)
[5] S. Datta and B. Das *Appl. Phys. Lett.* **56**, 665 (1990)
[6] D. Loss and D. P. DiVincenzo *Phys. Rev. A* **57**, 120 (1998)
[7] Y. A. Bychkov and E. I. Rashba, *J. Phys. C* **17**, 6039 (1984)
[8] G. Dresselhaus, *Phys. Rev.* **100**, 580 (1955)
[9] O. Voskoboynikov, C. P. Lee, and O. Tretyak, *Phys. Rev. B* **63**, 165306 (2001).
[10] C. F. Destefani, S. E. Ulloa and G. E. Marques, *Phys. Rev. B* **69**, 125302 (2004)
[11] D. Bulaev and D. Loss, *Phys. Rev. B* **71**, 205324 (2005)
[12] S. Takahashi, R. S. Deacon, K. Yoshida, A. Oiwa, K. Shibata, K. Hirakawa, Y. Tokura and S. Tarucha, *Phys. Rev. Lett.* **104**, 246801 (2010).
[13] A. J. Bennett, M. A. Pooley, Y. Cao, N. Sköld, I. Farrer, D. A. Ritchie and A. J. Shields, *Nat. Commun.* **4**, 1522 (2013)
[14] M. P. Nowak, B. Szafran, F. M. Peeters, B. Partoens and W. J. Pasek, *Phys. Rev. B* **83**, 245324 (2011).
[15] Y. Kanai, R. S. Deacon, S. Takahashi, A. Oiwa, K. Yoshida, K. Shibata, K. Hirakawa, Y. Tokura and S. Tarucha, *Nat. Nanotechnol.* **6**, 511 (2011)
[16] S. Takahashi, R. S. Deacon, A. Oiwa, K. Shibata, K. Hirakawa and S. Tarucha, *Phys. Rev. B* **87**, 161302 (2013)
[17] R. Winkler, *Spin-Orbit Coupling Effects in Two-Dimensional Electron and Hole Systems* (Springer, Berlin, 2003)
[18] T. K. Johal, R. Rinaldi, A. Passaseo, R. Cingolani, A. Vasanelli, R. Ferreira and G. Bastard, *Phys. Rev. B* **66**, 075336 (2002)
[19] I. Vurgaftman, J. R. Meyer and L. R. Ram-Mohan, *J. Appl. Phys.* **89**, 5815 (2001)
[20] M. Müller, A. Cerezo, G. D. W. Smith, L. Chang and S. S. A. Gerstl, *Appl. Phys. Lett.* **92**, 233115 (2008)
[21] A. D. Giddings, J. G. Keizer, M. Hara, G. J. Hamhuis, H. Yuasa, H. Fukuzawa and P. M. Koenraad, *Phys. Rev. B* **83**, 205308 (2011)
[22] See supplementary material for S. Takahashi, R. S. Deacon, K. Yoshida, A. Oiwa, K. Shibata, K. Hirakawa, Y. Tokura and S. Tarucha, *Phys. Rev. Lett.* **104**, 246801 (2010).
[23] J. van Bree, A. Yu. Silov, P. M. Koenraad, M. E. Flatté and C. E. Pryor *Phys. Rev. B* **85**, 165323 (2012)
[24] P. Stano, and J. Fabian, *Phys. Rev. Lett.* **96**, 186602 (2006).
[25] J. M. Garcia, T. Mankad, P. O. Holtz, P. J. Wellman, and P. M. Petroff, *Appl. Phys. Lett.* **72**, 3172 (1998).
[26] Z.R. Wasilewski, S. Fafard, and J.P. McCaffrey, *J. Cryst. Growth* **201-202**, 1131 (1999).